Where is 'Dorsal V4' in Human Visual Cortex? Retinotopic, Topographic and Functional Evidence

Roger B.H. Tootell and Nouchine Hadjikhani

Nuclear Magnetic Resonance Center, Department of Radiology, Massachusetts General Hospital, Charlestown, MA 02129, USA

In flattened human visual cortex, we defined the topographic homologue of macaque dorsal V4 (the 'V4d topologue'), based on neighborhood relations among visual areas (i.e. anterior to V3A, posterior to MT+, and superior to ventral V4). Retinotopic functional magnetic resonance imaging (fMRI) data suggest that two visual areas ('LOC' and 'LOP') are included within this V4d topologue. Except for an overall bias for either central or peripheral stimuli (respectively), the retinotopy within LOC and LOP was crude or nonexistent. Thus the retinotopy in the human V4d topologue differed from previous reports in macaque V4d. Unlike some previous reports in macaque V4d, the human V4d topologue was not significantly color-selective. However, the V4d topologue did respond selectively to kinetic motion boundaries, consistent with previous human fMRI reports. Because striking differences were found between the retinotopy and functional properties of the human topologues of 'V4v' and 'V4d', it is unlikely that these two cortical regions are subdivisions of a singular human area 'V4'.

Introduction

It is difficult to be certain whether a given cortical area in humans is homologous to a specific cortical area in a different species, such as macaque monkeys. In this example, the two species have evolved independently from each other over ~30 million years. The evolution of the cortical maps during this time cannot be reconstructed, since the cortical maps left no fossil record. Thus any assertion of homology between two such candidate cortical areas is ultimately inferential.

Despite this uncertainty, certain cortical areas are widely accepted as homologous across species, based on multiple lines of circumstantial evidence (Baker *et al.*, 1981; Kaas and Krubitzer, 1991; Sereno and Allman, 1991; Rosa *et al.*, 1993; Kaas, 1995; Rosa and Krubitzer, 1999) (D.C. Van Essen *et al.*, submitted for publication). In the visual cortex (one of the most well-mapped cortical regions), the kinds of evidence used to infer homology between candidate areas in two species include similarities in: (i) functional properties; (ii) retinotopy; (iii) patterns of intra-cortical connections; (iv) histological and biochemical features; and (v) topography. Based on three of these criteria (functional properties, retinotopy and topography), several visual cortical areas have already become accepted as homologous, in comparisons between macaque maps and functional magnetic resonance imaging (fMRI)-based human maps (Sereno *et al.*, 1995a; Tootell *et al.*, 1995, 1997; DeYoe *et al.*, 1996; Wandell, 1999). Such human areas include areas V1, V2, V3/VP, V3A and MT+. Earlier positron emission tomography (PET) data first suggested a likely human homologue of monkey area MT (Lueck *et al.*, 1989; Zeki *et al.*, 1991; Watson *et al.*, 1993).

Although this list includes homologues of most of the well-studied areas in macaque visual cortex (e.g. V1, V2 and MT), one glaring omission is macaque area V4. Macaque V4 has been well-studied with regard to spatial filtering properties (Desimone and Schein, 1987; Gallant *et al.*, 1993; Cheng *et al.*, 1994; Connor *et al.*, 1996; McAdams and Maunsell, 2000), color (Zeki, 1973, 1977, 1978; Van Essen and Zeki, 1978; Fischer *et al.*, 1981; Schein *et al.*, 1982; Schein and Desimone, 1990), extraretinal modulation (Moran and Desimone, 1985; Haenny *et al.*, 1988; Motter, 1993; Connor *et al.*, 1996, 1997), and models of visual processing (Gochin, 1994; Niebur and Koch, 1994; Courtney *et al.*, 1995; Salinas and Abbott, 1997; Bar and Biederman, 1999; Wilson *et al.*, 2000). V4 also occupies a critical position in the cortical hierarchy; it is often regarded as a 'gatekeeper' in the chain of 'ventral stream' areas extending into inferotemporal cortex (Maunsell and Newsome, 1987; Felleman and Van Essen, 1991b; Van Essen and Gallant, 1994). Unlike neighboring area MT, V4 receives roughly balanced inputs from both magnocellular and parvocellular streams (Ferrera *et al.*, 1992, 1994).

Macaque V4 is often subdivided into dorsal and ventral sub-areas (V4d and V4v, respectively), which include retinotopic representations of the lower and upper visual field, respectively (see Fig. 1). In humans, retinotopic and topographic evidence from fMRI has revealed the apparent homologue of ventral V4 ('V4v'), in several laboratories (Sereno *et al.*, 1995a; DeYoe *et al.*, 1996; Tootell *et al.*, 1997; Grill-Spector *et al.*, 1998b; Hadjikhani *et al.*, 1998; Baseler *et al.*, 1999; Wandell, 1999). However, the human homologue of macaque dorsal V4 ('V4d') has not yet been systematically described.

This is potentially quite important, because almost all of the data from macaque 'V4' has in fact been acquired from dorsal V4, not ventral V4. Experimentally, dorsal V4 is much more accessible than ventral V4. This distinction between V4d and V4v would be irrelevant, if these two cortical regions are in fact two retinotopic subdivisions of the same functional area, as currently assumed. However, at least in human visual cortex, our data suggest that these two cortical regions ('V4v' and 'V4d') appear to be distinctly different cortical areas, rather than two retinotopic subdivisions of the same area.

Here we describe these and related fMRI results, which were originally designed to reveal a homologue of macaque 'dorsal V4' in human visual cortex. As described above, the results of these tests turned out quite different than we expected. Our fMRI results strongly suggest that the human cortical visual area located where V4d should be (the V4d 'topologue') does not correspond to previous descriptions of dorsal V4 in macaques, neither retinotopically nor functionally. Unlike human V4v, the human V4d topologue is not retinotopically well differentiated, although it can be subdivided into two eccentricity-based subdivisions.

These unexpected results in the human V4d topologue may indicate that a significant species difference exists between macaque and humans. This would not be terribly surprising,

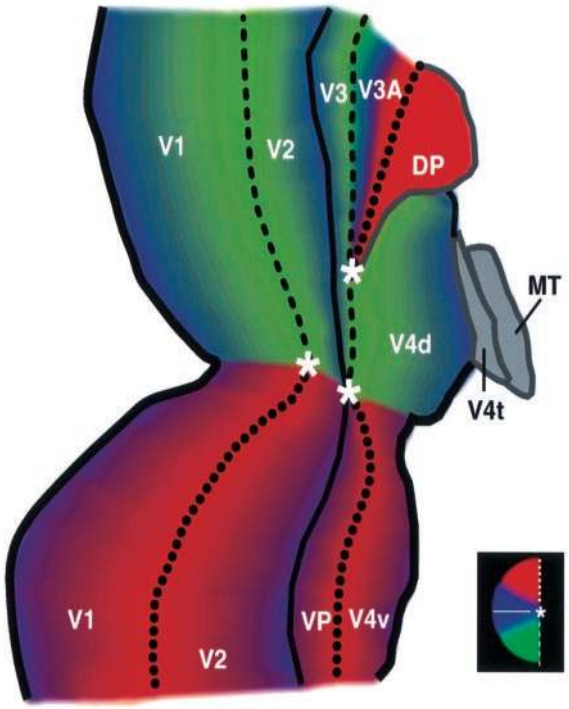

Figure 1. Diagram of the retinotopic organization of macaque area V4 and neighboring areas. The diagram is drawn in flattened cortical format, from a right hemisphere. Representations of the fovea (at the V1/V2 and V3/VP/V4 borders, and in V3A) are indicated with an asterisk. Within each area, increasingly peripheral eccentricities are represented at increasingly distant locations from those asterisks, approximately perpendicular to the lines of iso-polar angle. Lines of iso-polar angle are mapped roughly as radii from the foveal asterisks (see red, blue and green logo on the bottom right). Representations of the horizontal meridia are indicated using solid black lines, and representations of the upper and lower vertical meridian are indicated with dotted and dashed black lines, respectively. Areas and area boundaries which are not well-defined retinotopically, or not relevant here, are indicated using gray. Previously published maps all agree on the retinotopy of macaque areas V1, V2 and V3/VP. However, the descriptions of retinotopy and area borders can differ in reports from increasingly more anterior (generally, higher-order) areas. Thus the retinotopy in V3A in Gattass *et al.* (Gattass *et al.*, 1988) differs slightly from that described by Van Essen and colleagues (Van Essen *et al*., 1990, 1992; Felleman and Van Essen, 1991b). Similarly, area 'DP' is included in the maps of some groups (Andersen *et al*., 1985; May and Andersen, 1986; Felleman and Van Essen, 1991b), but not in the maps drawn by others (Gattass *et al*., 1988; Colby and Duhamel, 1991). Early retinotopic studies of V4 by one group (Baizer and Maguire, 1983; Maguire and Baizer, 1984) were inconsistent with a single retinotopic area. Many of those apparent discrepancies were later rationalized by Gattass *et al*. (Gattass *et al*., 1988). Where previous reports differ from each other, we have incorporated the data that are most cited, most recent, and/or best documented. The dorsal and ventral subdivisions of V4 (V4d and V4v, respectively) are largely separate from each other. V4d and V4v border each other only at the foveal representation, and diverge increasingly at the representation of progressively greater eccentricities. This 'bisected' arrangement is similar to that found in V2 and V3/VP. Thus in V4d, the fovea is represented inferiorly, and increasing visual field eccentricity is mapped superiorly and anteriorly, between V3A and MT. According to current views, V4d includes a representation of just the lower visual field, not the upper. In one previous report (Gattass *et al*., 1988), a portion of the upper visual field near the horizontal meridian was also included in V4d, instead of V4v. This unusual upper field representation was later attributed instead to adjacent area TEO (Boussaoud *et al*., 1991), and this figure adopts that assumption. The 'field sign' (Sereno *et al*., 1994, 1995b) in both V4 subdivisions matches the visual field geometry, as in V2 (thus, opposite to the mirror-symmetric field signs found in V1 and V3/VP).

since cortical maps have evolved into quite different forms, based on comparisons between other primates – especially in the higher-tier areas beyond V1 and V2. Many of the cortical visual areas in other well-mapped primate species (e.g. aotus monkey and galago) have no obvious counterpart in macaque (Kaas, 1995; Rosa and Krubitzer, 1999). It is arguable whether a 'V4' homologue even exists in non-human primates other than macaque (Felleman and Van Essen, 1991b; Kaas and Krubitzer, 1991; Sereno and Allman, 1991; Rosa *et al*., 1993; Kaas, 1995; Rosa and Krubitzer, 1999).

Alternatively, it is possible that human-like retinotopic and functional distinctions also exist between V4v and V4d in macaques, which have not yet been widely recognized (Steele *et al*., 1991; Stepniewska and Kaas, 1996). Irrespective of how this matter is eventually resolved, it is significant, since the topographical organization of macaque visual cortex is often used as a model for that in human visual cortex.

V4 and Color Processing

The localization of V4 has special importance because it has been claimed that V4 processes color information selectively. The original report was that all (Zeki, 1973) or a majority (Zeki, 1977, 1978) of cells in (dorsal) V4 are wavelength-selective. However, when more systematic studies began considering the effects of stimulus variations in luminance as well as color, and measuring color responses quantitatively, the reported percentage of wavelength-selective cells in V4 decreased to levels which were similar to those in neighboring cortical areas (Fischer *et al*., 1981; Schein *et al*., 1982). A more recent report (Schein and Desimone, 1990) confirmed that the percentage of classic opponent-color cells was small in V4, but it also allowed for some higher-order processing of wavelength information over wide regions of the visual field (e.g. color constancy). On the other hand, similar responses to wide-field color changes have been reported in macaque V1 (Wachtler *et al*., 1997, 1998, 1999a,b), so there may be nothing unique about the wide-field color responses in V4.

A similar conclusion was reached by lesion studies. Across a range of laboratories, lesions of macaque V4d had little effect on behavioral tests of wavelength discrimination (Schiller, 1993; Walsh *et al*., 1993) (W. Merrigan, personal communication). Even lesions that apparently included ventral V4 did not produce achromatopsia (Heywood *et al*., 1992). In one lesion study including V4 (Walsh *et al*., 1993), deficits were reported in the processing of color constancy. However such effects could also (or instead) reflect secondary effects of brain lesions on higher-tier areas to which V4 projects (e.g. pIT; see below), rather than a direct effect in V4.

Other evidence suggests that a different area of macaque visual cortex is homologous to the area implicated in human achromatopsia. That revised color-selective area is located anterior and ventral to V4, in-or-near posterior inferotemporal (pIT) cortex, perhaps in areas PIT or TEO (see Fig. 2). The evidence for this includes the following. First, when pIT is lesioned, prominent deficits are seen in wavelength sensitivity (Heywood *et al*., 1995) (W. Merrigan, personal communication), unlike the lack of such deficits following V4 lesions. Secondly, this pIT region shows higher brain activity in neuroimaging experiments, when macaques are performing wavelength discriminations (Takechi *et al*., 1997). Finally, pIT corresponds to the region which should be color-selective in macaques, based on the topography of color-selective areas in human visual cortex (see below; cf. Figs 2 and 3).

Overall, these data do not constitute a persuasive case for color selectivity in macaque V4. Despite this, a small color-selective region which was discovered in human visual cortex was initially named 'human V4' (Lueck *et al*., 1989). Subsequent retinotopic studies revealed that this color-selective region ('V8',

'VO' or 'V4', in different accounts) is actually located in an area anterior to human area V4v (Hadjikhani *et al.*, 1998) (see Fig. 3).

A subsequent controversy developed about the details of the retinotopy and the localization of this color-selective region, relative to human V4v (Tootell and Hadjikhani, 1998; Zeki *et al.*, 1998; Bartels and Zeki, 2000). However, these arguments are misleading, since the original claims for color selectivity in single unit reports were acquired from dorsal V4, not ventral V4 (see Figs 2 and 3). Thus the real issue is whether the small color-selective region described in ventral human visual cortex could possibly be homologous to dorsal V4, not ventral V4. This appears unlikely, based on the cortical topography (see Figs 2 and 3) and other factors (see below). As described above, this distinction becomes especially important if V4d and V4v are actually distinct cortical areas with inappropriately similar names, rather than two retinotopic subdivisions of a single visual area. Such tests were the focus of this report.

Materials and Methods

The methods in this study were similar to those described elsewhere (Sereno *et al.*, 1995a; Tootell *et al.*, 1997, 1998; Hadjikhani *et al.*, 1998). Informed written consent was obtained from each subject prior to the scanning session, and all procedures were approved by Massachusetts General Hospital Human Studies protocol no. 96-7464. Normal human subjects, with (or corrected to) emmetropia, were scanned in a high field (3 T) General Electric magnetic resonance (MR) scanner retrofitted with echo-planar imaging (ANMR Corp.). Head motion was minimized by using bite bars with deep, individually molded dental impressions. The subject's task was to continuously fixate the center of all visual stimuli throughout the scan acquisition.

Magnetic resonance images were acquired using a custom-built quadrature surface coil, shaped to fit the posterior portion of the head. Magnetic resonance slices were 3–4 mm thick, with an in-plane resolution of 3.1 × 3.1 mm. Each scan took either 8 min 32 s (retinotopy), or 4 min 16 s (all other scans), using a TR of either 4 or 2 s, respectively. Each scan included 2048 images, consisting of 128 images per slice in 16 contiguous slices.

Phase-encoded retinotopic maps were obtained from 41 subjects (115 scans polar angle, 115 scans eccentricity, 471040 images total). Additional area-labeling scans (49 scans, 100352 images) were also acquired to clarify the location of MT+ and other visual areas. Among these subjects, 14 were also tested for sensitivity to color-versus-luminance, color afterimages, and sensitivity to kinetic boundary stimuli (216 scans, 442368 images total).

All stimuli were projected onto a screen located ~24 cm from the subjects' eyes, using a LCD projector (NEC, model MT 800; 800 × 600 pixel resolution). Stimuli for retinotopic mapping were slowly moving, phase-encoded thin rays or rings comprised of counterphasing checks, which varied semi-randomly in both luminance and color. For a given subject, retinotopic information was signal-averaged from 4–12 scans (8192–24576 images) of polar angle or eccentricity. Data were also combined from different slice prescriptions on the same cortical surface, to reduce intervoxel aliasing. The retinotopic stimuli extended from 0.2° to 18°/25°/30° into the periphery, along the vertical/horizontal/oblique axes, respectively (thus up to 60° in visual extent).

Cortical Flattening and Spatial Filtering

For each subject, a first step was to acquire the structural MR images needed for reconstruction. Such acquisitions were optimized for contrast between gray and white matter in brain, and these procedures are described in full elsewhere (http://www.nmr.mgh.harvard.edu/freesurfer) (Sereno *et al.*, 1995b; Dale *et al.*, 1999; Fischl *et al.*, 1999). This structural scan was acquired only once per subject, in a head coil for full head coverage.

From these three-dimensional data, image components caused by the skull were stripped off automatically by 'shrink-wrapping' a stiff deformable template onto the brain images. Then the gray–white matter boundary was estimated for each hemisphere with a region-growing method. The result was tessellated to generate a surface (~130 000 vertices) that was refined against the MRI data with a deformable template algorithm. Then it was inspected for topological defects (e.g. 'handles') and reconstructed without surface defects, if necessary.

The resulting surface was aligned manually with the functional scan by direct iterative comparisons in three orthogonal planes between the echo-planar imaging (EPI) inversion recovery scan (1.5 × 1.5 × 3–4 mm) and the high-resolution data set (1 × 1 × 1 mm) used to construct the cortical surface. By choosing a surface centered on the gray–white matter boundary, we effectively sampled activity most in cortical layers 4–6, rather than near the surface where the macrovascular artifact is maximal. Thus it was possible to assign activity more accurately to the correct bank of a given sulcus. The lower resolution activation data (3 × 3 × 3–4 mm) was interpolated smoothly onto the higher-resolution surface polygon (one polygon ~1 × 1 mm). Then the surface was unfolded by reducing curvature while adding an additional area-preserving term. For a completely flattened cortical surface, the inflated brain was cut along the calcarine fissure and just posterior to the sylvian fissure. The resulting surface was pushed onto a coronal plane in one step and unfurled on the plane. A relaxation algorithm was applied to minimize areal and linear distortion, weighted equally. The vertex update rule for flattening was further modified to include a shear-minimizing term, because maintaining only the original local areas allows substantial distortion (e.g. rectangular and rhombic distortions of an original square). After flattening, the data was spatially smoothed using a kernel of ~2.5 mm (half-amplitude at half-maximum).

In some analyses, we sampled values of retinotopic phase across the flattened cortical surface, in one-dimensional plots. In such analyses, data were plotted for each vertex crossed in the flattened cortical surface, along a line which was as straight as possible between adjacent vertices.

The V4d Topologue

We tested for a 'V4d' in human visual cortex by first delineating the cortical region in which V4d should be located (i.e. by creating a V4d 'topologue'), in each human subject tested. This 'topologue' approach assumes that neighborhood relationships between cortical areas tend to be conserved during evolution. For example, it assumes that area V2 in a given species does not arbitrarily disengage itself from adjacent areas V1 and V3 during evolution, then move a long way across cortex, to re-settle itself in some random location far anteriorly. This assumption is well supported by empirical comparisons of cortical visual maps across multiple species of non-human primate (Baker *et al.*, 1981; Sereno *et al.*, 1994; Kaas, 1995; Rosa and Krubitzer, 1999), and by theories of cortical development (Van Essen, 1997). The location of our V4d topologue was not constrained by the location of specific sulci and gyri, since the existence of specific gyri and sulci (and their relationship to corresponding visual areas) can vary greatly between species.

According to all published accounts, macaque V4d is located: (i) superior to the cortical region called 'V4v'; (ii) anterior to V3A; and (iii) posterior to MT (and the small transition area 'V4t') (see Figs 1 and 2). Therefore, we defined our human V4d topologue so that it was also located: (i) superior to human V4v; (ii) anterior to V3A; and (iii) posterior to human area 'MT+' (see Fig. 3). Human 'MT+' is presumed homologous to human MT plus small adjacent motion-selective areas (DeYoe *et al.*, 1996).

This was essentially a topographic analysis. Thus, the V4 topologue was defined on a two-dimensional cortical surface which could be displayed in either normal, inflated or flattened mode (e.g. Figs 2 and 3).

Results

Stereotaxic Localization

The Talairach coordinates for the center of our V4d topologue were: +/–41.25, –81, 8 (SD 5.85, 3.46, 2.71) (Talairach and Tournoux, 1988).

Retinotopy

Next we tested whether the fMRI retinotopy in our V4d topologue matched the retinotopy predicted above (e.g. Fig. 1).

At first glance, the human maps of retinotopic eccentricity in the V4d topologue seemed to match the retinotopic predictions of macaque V4d, and V4v in both humans and macaques. As illustrated in Figure 4, the near-foveal stimuli produced preferential activity in the inferior and posterior corner of our V4d topologue, near the confluent foveal representation of V4v, V3/VP, etc. More peripheral retinotopic stimuli activated the V4d topologue further anterior and superiorly, between MT+ and V3A.

However, closer inspection revealed that the representation of retinotopic eccentricity was unusual in this V4d topologue. The representation of parafoveal eccentricities (rendered in blue) here was unusually (sometimes vanishingly) thin. In contrast, activation produced by stimuli at central eccentricities (rendered in red) and more peripheral eccentricities (rendered in green) was robust and extensive (see Fig. 4). By comparison, in the classical retinotopic areas (e.g. V1, V2, V3/VP, etc.), there was a significantly larger representation of the middle eccentricities (see blue band in those areas in Fig. 4), as one would expect from previous measurements of the cortical magnification in other cortical areas (Engel *et al.*, 1994, 1997; Sereno *et al.*, 1995b) and other primate species (Daniel and Whitteridge, 1961; Hubel and Wiesel, 1974; Van Essen *et al.*, 1984; Tootell *et al.*, 1988). This was our first hint that the eccentricity representation is anomalous in the V4d topologue.

For convenience, we describe the cortical zone which responds preferentially to central visual stimuli as 'LOC' (Lateral Occipital Central), and the zone which responds preferentially to more peripheral stimuli as 'LOP' (Lateral Occipital Peripheral). The anomalous nature of the eccentricity map in LOC/LOP was revealed more clearly by measuring the representation of optimal stimulus eccentricity, in one-dimensional plots measured across the cortical surface. As shown in Figure 5*B* (bottom row), responses in the V4d topologue were biased for either central or peripheral stimuli (in LOC or LOP, respectively), without the typical monotonic gradations of eccentricity sensitivity seen in V1, V2, V4v and other classically retinotopic areas (Fig. 5*B*, top row). In most of these one-dimensional samples, we found little systematic variation in the maps of stimulus eccentricity within either LOC or LOP. Instead, there was a pronounced discontinuity at the border between LOC and LOP.

Two alternative hypotheses arise from this data. First, LOC and LOP could be two parts of the same visual area, like centrally and peripherally driven regions in classical retinotopic areas, but (for unknown reasons) the representation of eccentricities from ~0.5 to 4° is systematically compressed or absent.

An alternative hypothesis is that LOC and LOP are two distinct cortical areas, located adjacent to each other, but lacking internal retinotopy in either area. This second hypothesis requires furthermore that LOC is driven most effectively by stimuli from the central visual field, and that LOP is driven preferentially by stimuli in more peripheral visual field regions. Similar eccentricity-based biases have been reported previously in other visual areas (Allman and Kaas, 1976; Cusick and Kaas, 1988; Stepniewska and Kaas, 1996).

The first hypothesis is a complicated modification of classical retinotopic maps, like these in V1, V2, V3, V3A. The second hypothesis is driven more by the actual data—such as the relative lack of internal retinotopy within each of LOC and LOP, and the pronounced retinotopic discontinuity between them (e.g. Figs 4 and 5).

This choice between these two hypotheses can be narrowed down by testing the mapping of retinotopic polar angle in the V4d topologue. If there is a lack of eccentricity retinotopy within LOC and LOP (the second hypothesis), we would expect a noisy, inconsistent polar angle selectivity—or none at all—in LOC and LOP. Hypothesis no. 1 would instead predict a systematic, classical polar angle representation of the lower visual field spanning the V4d topologue, as in Figure 1.

In contrast to the mapping of retinotopic eccentricity, the polar angle retinotopy in the V4d topologue was variable across subjects (e.g. Fig. 6). In this region, we did not find any consistent relationship between the human fMRI maps, relative to the polar angle retinotopy predicted in Figure 1. On balance, we conclude that the polar angle retinotopy supported hypothesis no. 2: LOC and LOP appear to be separate cortical areas, each with little systematic internal retinotopy, rather than something akin to macaque V4d.

It might be argued that the retinotopic differences illustrated in Figures 4–6 are based on idiosyncratic differences between individual maps, rather than true biological variations that remain consistent across individuals. In order to test this quantitatively, and across subjects, we sampled values of both retinotopic eccentricity and polar angle, from all 12 of the hemispheres (six subjects) in which the retinotopic maps were statistically most robust. The variations in eccentricity were measured in the V4d topologue along lines which were topographically similar to those shown in Figure 5 – approximately perpendicular to the lines of iso-eccentricity (or more accurately in this region, the two zones of foveal or peripheral retinotopic bias). This would be the appropriate way to measure such eccentricity variations, in classically retinotopic areas (e.g. Fig. 5*B*, top row of graphs).

For comparison, we also measured variations in retinotopic polar angle in the V4d topologue, along lines which were oriented approximately parallel to the lines of constant retinotopic eccentricity. To maximize consistency, the end-points of these sampling lines were set at the inferior V3A–V7 intersection on the posterior side, and at the inferior intersection of V4d with MT+ on the anterior side.

As shown in Figure 7*A*, these averaged values of retinotopic eccentricity show the same behavior as the individual samples shown in Figure 5. The central and peripheral biases were statistically different (average standard deviation = 24.6°). On the other hand, our averaged values of retinotopic polar angle showed no coherent pattern (i.e. the mean phase angles appear randomly distributed), with standard deviations which were correspond- ingly larger (SD = 104.5°). Thus this group-averaged data confirmed the retinotopic conclusions we reached earlier, from examination of the individual maps (e.g. Figs 4–6).

Functional Specialization

Using fMRI, we could also test whether the human V4d topologue responded preferentially to functional stimuli like those suggested by earlier electrophysiological reports in macaque V4d. For instance, does the human V4d topologue respond preferentially to color-varying stimuli?

In previous fMRI experiments (Hadjikhani *et al.*, 1998), we tested for color-selective activity throughout human visual cortex, using two types of color-selective tests. Such tests did produce preferential color-selective activity in some expected locations, including a site in the collateral sulcus that had been described previously (Lueck *et al.*, 1989), which may be involved in the syndrome of achromatopsia. However, such tests did not reveal preferential color-selective activity in the V4d

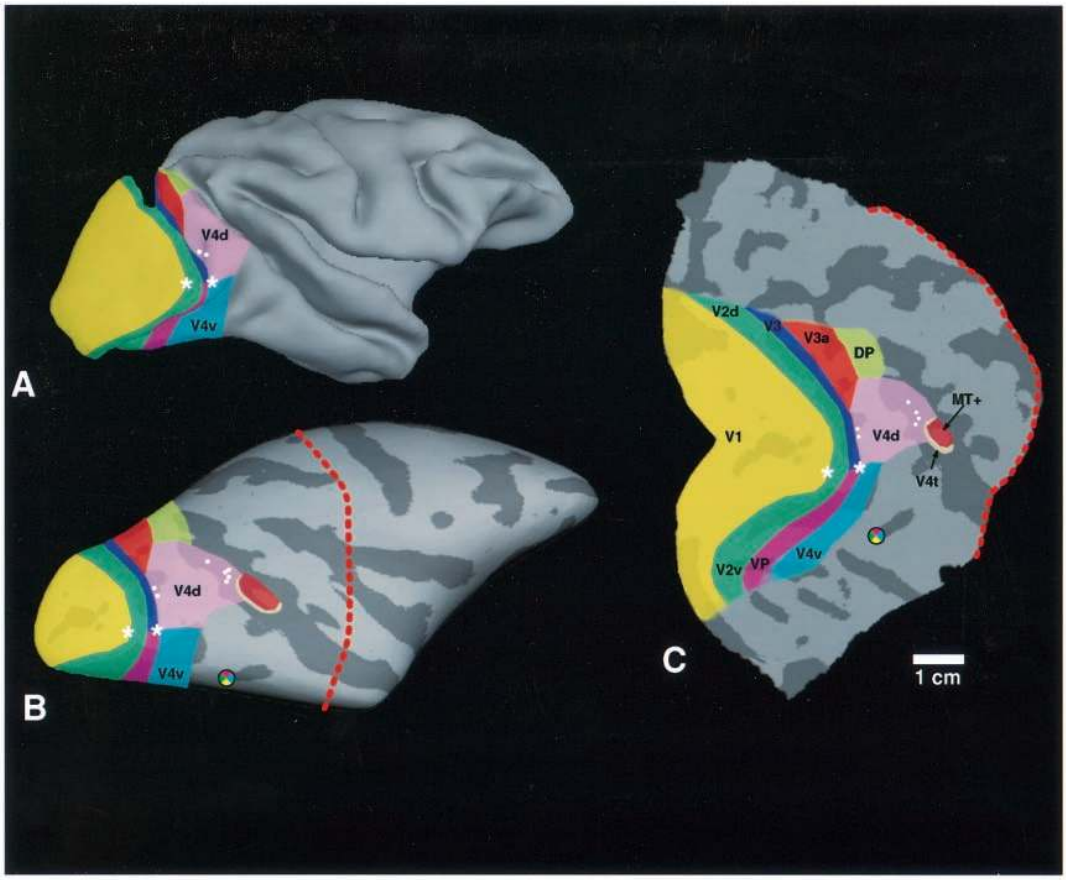

Figure 2

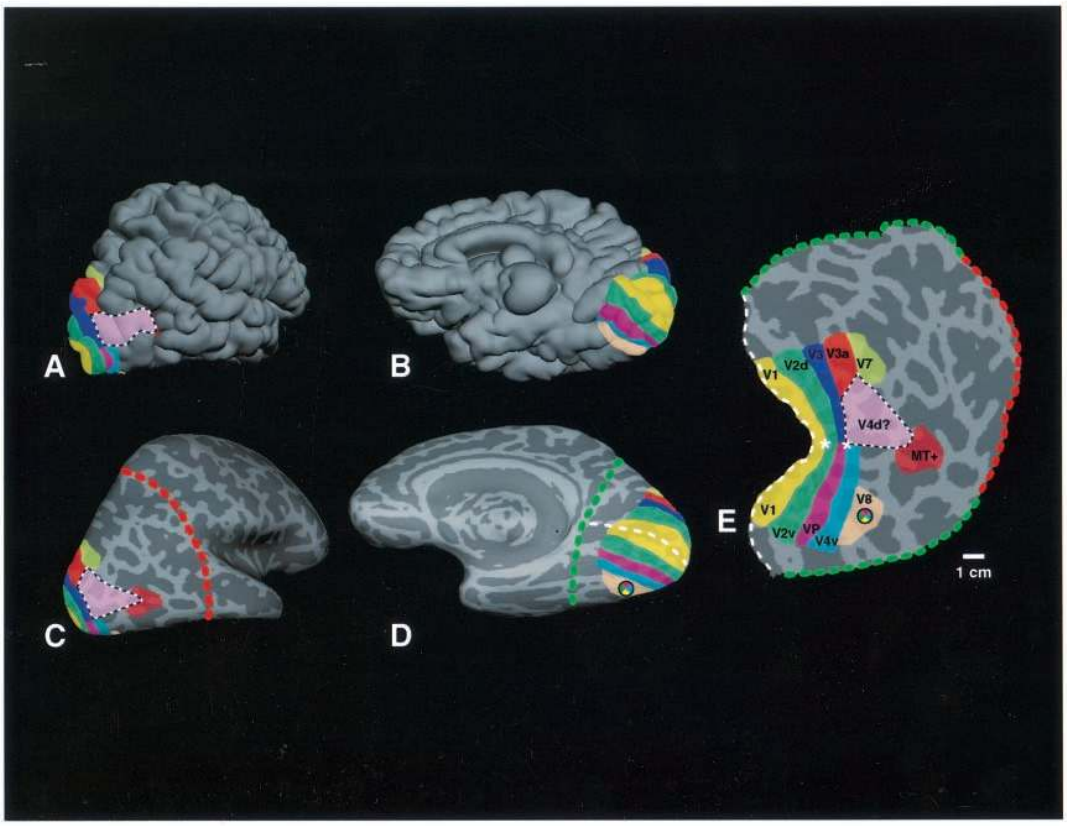

Figure 3

topologue (e.g. Fig. 8). At least in this set of tests, the V4d topologue did not appear to be color-selective.

Previous fMRI reports suggested a quite different kind of functional specialization in the human V4d topologue. Orban and co-workers have reported that an area which is apparently co-extensive with our V4d topologue (which they named 'KO') responds selectively to kinetic motion boundaries (Orban *et al.*, 1995; Dupont *et al.*, 1997; Van Oostende *et al.*, 1997).

To test whether our V4d topologue would respond selectively to kinetic motion boundaries, we used copies of the same stimuli used by the Orban group to reveal where that activity was located, relative to our phase-mapped retinotopic boundaries on the flattened cortex. As shown in Figure 9, our V4d topologue did respond selectively to the kinetic motion boundaries, consistent with earlier reports (Orban *et al.*, 1995; Dupont *et al.*, 1997; Van Oostende *et al.*, 1997). The kinetic motion comparison also produced additional activity in human area MT+ (see Fig. 9).

Although the human topologue of dorsal V4 did respond selectively to the kinetic motion, ventral V4 did not (see Fig. 9). This is important because again, in this test, V4v and V4d appear

Figure 2. The topography of V4 and other areas in macaque visual cortex, in relationship to previous measures of color selectivity. All panels are from the same hemisphere. The area maps are shown on a near-normal (folded) cortex (*A*), and the 'inflated' cortical surface (*B*), from a lateral viewpoint (anterior/posterior = rightmost/leftmost in the figure, respectively). The posterior part of the cortex [(i.e. to the left of the dashed red line in (*B*)] is shown in (*C*), in the flattened cortical format. In (*B*) and (*C*), lighter and darker gray indicate regions of the cortical surface which are curved either convexly or concavely *in vivo* (thus, corresponding roughly to gyri or sulci, respectively). Representations of the fovea in V1/V2 and V3/VP/V4 are indicated with asterisks. The scale bar [bottom right, (*C*)] corresponds to 1cm in the flattened cortical surface, excepting uncorrected spatial distortion due to cortical flattening. The visual areas are labeled in (*C*), and the corresponding areas are indicated using common colors in (*A*) and (*B*). Each white dot in V4d indicates the approximate location where a significant patch of color-selective cells was reported in previous single unit studies (Zeki, 1973, 1977). Such receptive fields were almost always located in the lower visual field, which confirms that they were located in dorsal V4. In human visual cortex, multiple neuroimaging studies have revealed a small region of color-selective activity located in the collateral sulcus, which may be involved in the clinical syndrome of prosopagnosia. This area has been described variously as either 'V8' (Hadjikhani *et al.*, 1998), 'V4' (Lueck *et al.*, 1989) or 'VO' (Wandell, 1999). In this diagram of macaque areas, the colored 'pinwheel' logo indicates the location where the homologous color-selective area would be located, assuming that a homologous region exists in macaques, and that the neighborhood relationships between cortical areas are evolutionarily conserved between humans and macaques. An additional color-selective, non-retinotopic area has been described anterior to this in human cortex (Beauchamp *et al.*, 1999; Bartels and Zeki, 2000), but that anterior area is not considered here.

Figure 3. The topography of V4 and other areas in human visual cortex, in relationship to previous measures of color selectivity. In most respects, the format is similar to that shown in Figure 2. However, in human visual cortex, the map of corresponding areas is 'pulled' further back into the medial bank, as if it was a printed pattern on a two-dimensional sheet. Thus to illustrate analogous regions on the human cortical map, we show both medial and lateral views of the normal folded cortex in (*A*) and (*B*) and the inflated cortex in (*C*) and (*D*). The same cortex in the flattened cortical format is shown in (*E*). The location of the artificial 'cut' lines used to separate the flattened patch in (*E*) are shown in (*C*) and (*D*) (red, green and white dashed lines). The location and topography of the cortical areas were based on functional and anatomical MR tests in each subject. The scale bar in (*E*) indicates ~1 cm. Based on the topography of areas which border V4v in macaque (i.e. V3A, V4v, MT), the location where a V4d homologue would be located in human visual cortex (the V4d 'topologue') is bounded using dashed white/black lines, and filled in pink [(see (*E*)]. Area V4v is filled in dark blue. The location of the ventral color-selective area ('V8') is indicated in tan, including the color pinwheel logo. Anatomical studies suggest that a homologue of area V4t (the MT 'ring' or 'crescent') may also exist (Tootell *et al.*, 1985; Kaas and Morel, 1993; Tootell and Taylor, 1995); if so, it should lie along the border where MT+ meets the V4d topologue.

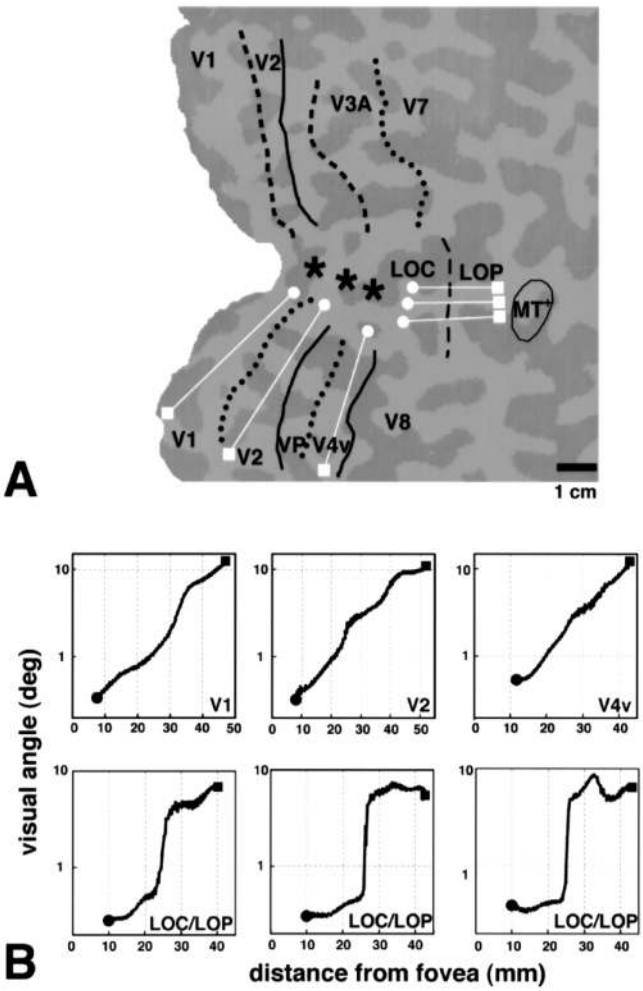

Figure 4. In the human V4d topologue, fMRI maps reveal an unusual representation of retinotopic eccentricity. (*A*)–(*D*) show phase-encoded maps of retinotopic eccentricity, produced by ring-shaped stimuli at systematically varied eccentricities, from two representative hemispheres. For ease of comparison, all examples are shown in right hemisphere format, but results were equivalent in both hemispheres. The top two maps, (*A*) and (*B*), had a cumulative spatial filtering of 2.5 mm (half-width at half-maximum), as elsewhere in the text. (*C*) and (*D*) show the same maps without this spatial post-processing. The 'pixelated' nature of the images in (*C*) and (*D*) reflects the acquisition voxel size (3 × 3 mm). The retinotopic area borders were based on an automated field sign analysis (Sereno, 1995). The stimuli were scaled in size and retinotopic position, consistent with a generalized cortical magnification factor (Sereno *et al.*, 1995b; Tootell *et al.*, 1997, 1998). Cortical regions showing relative increases to stimuli which were increasingly further from the fovea are coded in red, blue and green, respectively (see logo, bottom right). The calibration bar indicates ~1 cm. In such retinotopic maps, significant activity was typically absent from the very center of the foveal representation (i.e. the foveola), since an unchanging fixation spot occluded the retinotopic stimuli in that location. Thus it was necessary to estimate the area borders, and the representation of the foveola, within these signal-poor central regions. The limits of uncertainty near the foveal representation are indicated with a short white line crossing the iso-polar area borders. The V4d topologue is also drawn for each subject, using dashed white/black lines, as in Figure 3. In the classical retinotopic areas (e.g. V1, V2, V3/VP, V3A, V4v), this pseudocolor rendering of retinotopic eccentricity activity produced parallel bands of red > blue > green (when the stimuli were centered at visual field eccentricities of 1.6, 4.2 and 11.3°, respectively), with continuous and gradual transitions between them. However in the V4d topologue, there was a systematic under-representation of 'middle' eccentricities within our stimulus range. Thus the pseudocolor blue line was thin or absent in this region, in both the filtered and unfiltered maps [(e.g. (*A*)–(*D*)]. Much of the V4d topologue appeared to be activated preferentially by either foveal (red) or peripheral (green) stimulus eccentricities, as in classical retinotopic areas. For convenience, we call the centrally and peripherally activated regions 'LOC' and 'LOP', respectively.

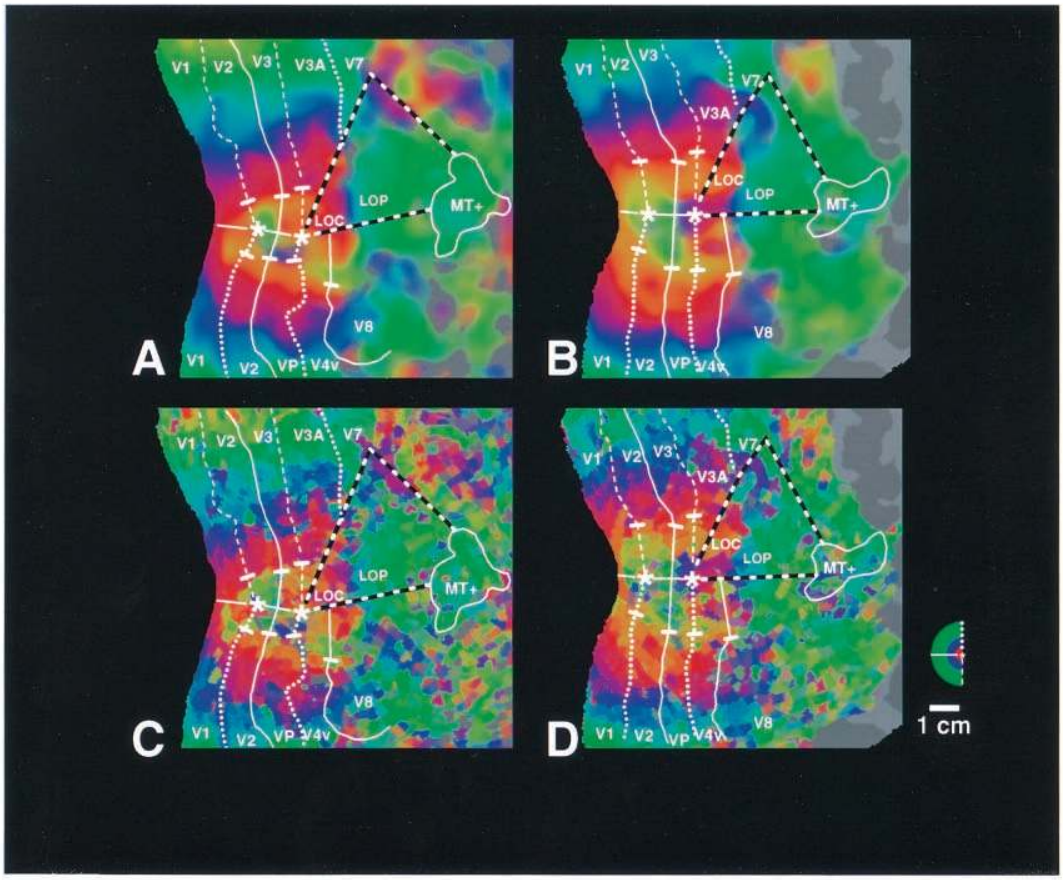

Figure 5

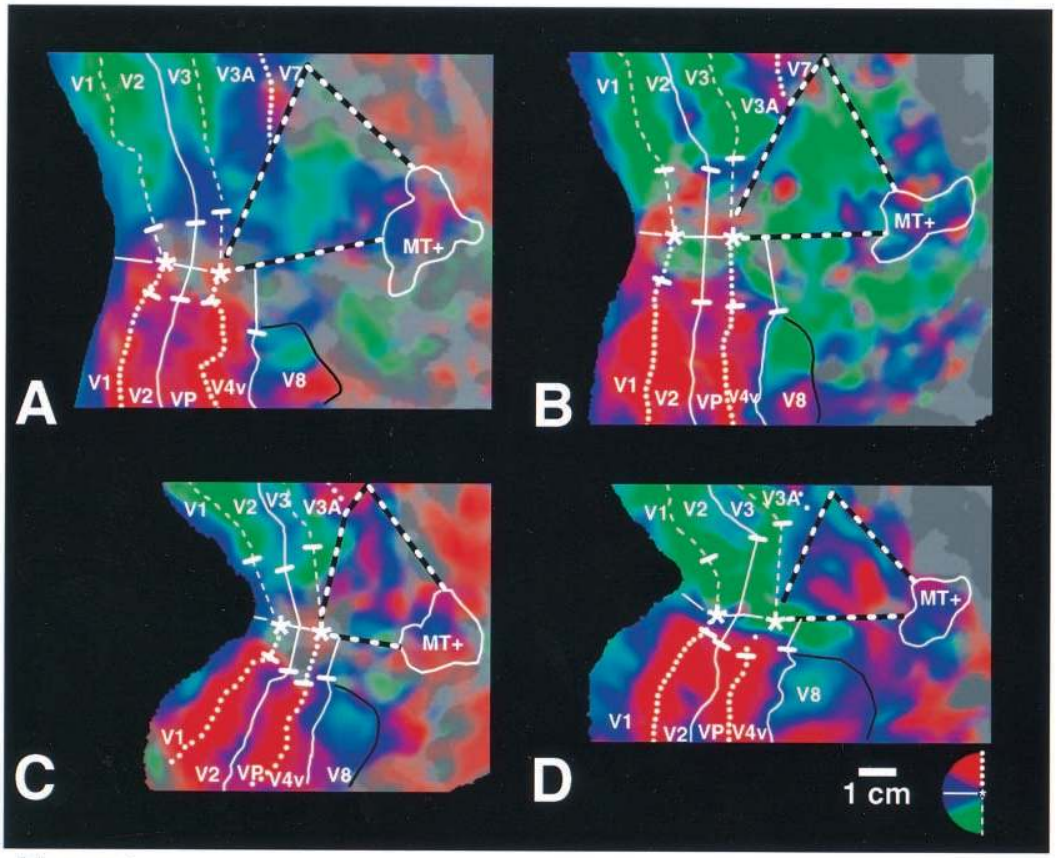

Figure 6

to be distinctly different areas, rather than two retinotopic subdivisions of a single inclusive area.

Discussion

We began this study with specific and limited aims: to confirm previous descriptions of macaque V4d, which we expected to find in corresponding parts of the human visual cortical map (i.e. the V4d 'topologue'). Instead, the fMRI evidence suggested either that (1) a V4d homologue does not exist in human visual cortex, or that (2) previous descriptions of function and retinotopy are inaccurate in macaque V4d.

Neither of our fMRI measures of retinotopy (neither eccentricity nor polar angle) matched the reported retinotopy of V4d in macaques. The retinotopic data in the V4d topologue was not even an appropriate lower field counterpart to the classical upper field representation in V4v—in neither humans nor macaques.

Furthermore, certain stimulus comparisons (e.g. kinetic motion boundaries) activated V4d but not V4v. Such functional differences between V4d and V4v are frankly incompatible with the definition of a single inclusive area 'V4'. As an analogy, if credible new studies revealed that motion selectivity were present in one half of area MT but not the other half, then the cortical maps would likely be redrawn to include two corresponding areas within the original area 'MT'.

Thus overall, there was very little support for (and much against) the hypothesis that a V4d homologue exists in the expected location in human visual cortex. However, is it possible that we somehow missed the 'real' human homologue of V4d? Does an actual homologue, with properties more similar to

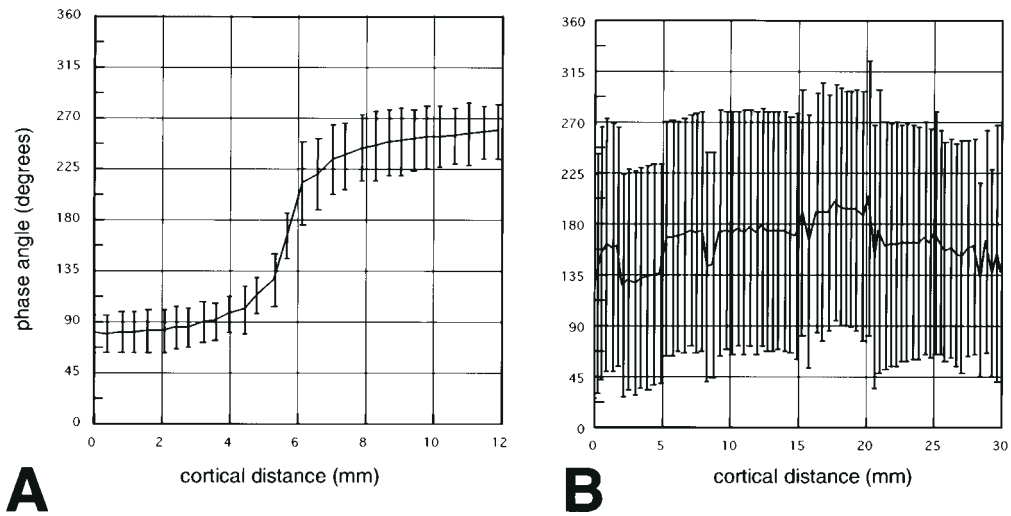

Figure 7. Averaged measurements confirm the unusual retinotopy in the human V4d topologue. One-dimensional measurements were made across the flattened (two-dimensional) cortical surface, along two axes in each of 12 hemispheres (six subjects). For each vertex along the cortical surface (converted to cortical distance, along the *x* axis), the corresponding retinotopic phase angle is shown on the *y* axis. The brackets indicate one standard error. (*A*) shows the averaged values measured in LOC/LOP as in Figure 5*B* (i.e. perpendicular to the border between the two eccentricity-biased zones). In a classically retinotopic area, this would be equivalent to making measurements of retinotopic eccentricity, along lines of constant iso-polar-angle. At smaller phase angles, the ring-shaped eccentricity-mapping stimulus was smaller and closer to the central fixation point (i.e. the foveal representation). At larger phase angles, the stimulus was correspondingly larger and further from the fixation point (stimulating more peripheral locations on the retina). Since the size of all the retinotopic areas varies in different subjects (mostly with corresponding variations in brain size), the length of individual samples in the averaged sample has been truncated to match the smallest of the sampled lines. Since the foveal and peripheral retinotopic limits were difficult to define, the samples have been aligned along the LOC/LOP border. (*B*) shows the averaged values along the orthogonal axis, measured roughly parallel to the LOC/LOP border. In classically retinotopic areas, this would comprise measurements of polar angle variations, made parallel to lines of constant eccentricity. Here, for consistency, the end-points of these sampling lines were set at the inferior V3A–V7 intersection on the posterior side [(left side of (*B*)], and at the inferior intersection of V4d with MT+ anteriorly (right side of graph).

Figure 5. One-dimensional measurements of optimal retinotopic eccentricity clarify the unusual representation of retinotopic eccentricity in LOC and LOP. (*A*) shows the map from which measurements were made, and the six corresponding measurements are shown in (*B*). As much as possible, measurements were made from lines running near-perpendicular to lines of constant eccentricity (white lines), from near-foveal representations (white circles), to more peripheral representations (white squares), with each measurement confined to a single cortical area/region. The calibration bar [bottom right, (*A*)] indicates ~1cm. Data from three classical retinotopic areas (V1, V2 and V4v) are shown in the top three graphs of (*B*). Such plots yielded continuous and near-exponential decreases in cortical magnification from increasingly peripheral visual field locations, consistent with earlier measures of the cortical magnification factor. However, analogous data from LOC/LOP were quite different. Measurements taken from LOC/LOP [(top-to-bottom in (*A*)] are shown from left-to-right, respectively, in (*B*). Within LOC or LOP, such data shows small, apparently random fluctuations in the optimal visual field location, from either the foveal region (<~0.5°) or from regions peripheral to ~4°, respectively. At the LOC/LOP border, there was a sharp discontinuity. Overall, such data suggest that there may be just two cortical areas (LOC and LOP), each with a complementary bias for stimuli in either foveal or peripheral eccentricities, with little or no systematic retinotopic gradient linking the two regions.

Figure 6. In the V4d topologue, the fMRI maps reveal a non-systematic representation of retinotopic polar angle, across different hemispheres. Each panel shows the polar angle maps from the same two hemispheres shown in Figure 4, plus two additional hemispheres to illustrate the range of results obtained. The figure format here is similar, except that the pseudocolor rendering is different. Here, red codes cortical regions which were preferentially activated by the upper visual field, blue for the polar angles spanning the horizontal meridian, and green for the lower visual field (see polar angle logo, bottom right). The spatial filtering here is equivalent to that in Figure 4*A*,*B*. Comparison of (*A*)–(*D*) shows that within the classical retinotopic areas (V1, V2, V3/VP, V3A and V4v), the polar angle retinotopy is quite consistent across subjects. However, in the V4d topologue (enclosed in white/black dashed lines), the polar angle maps vary between subjects, seemingly randomly.

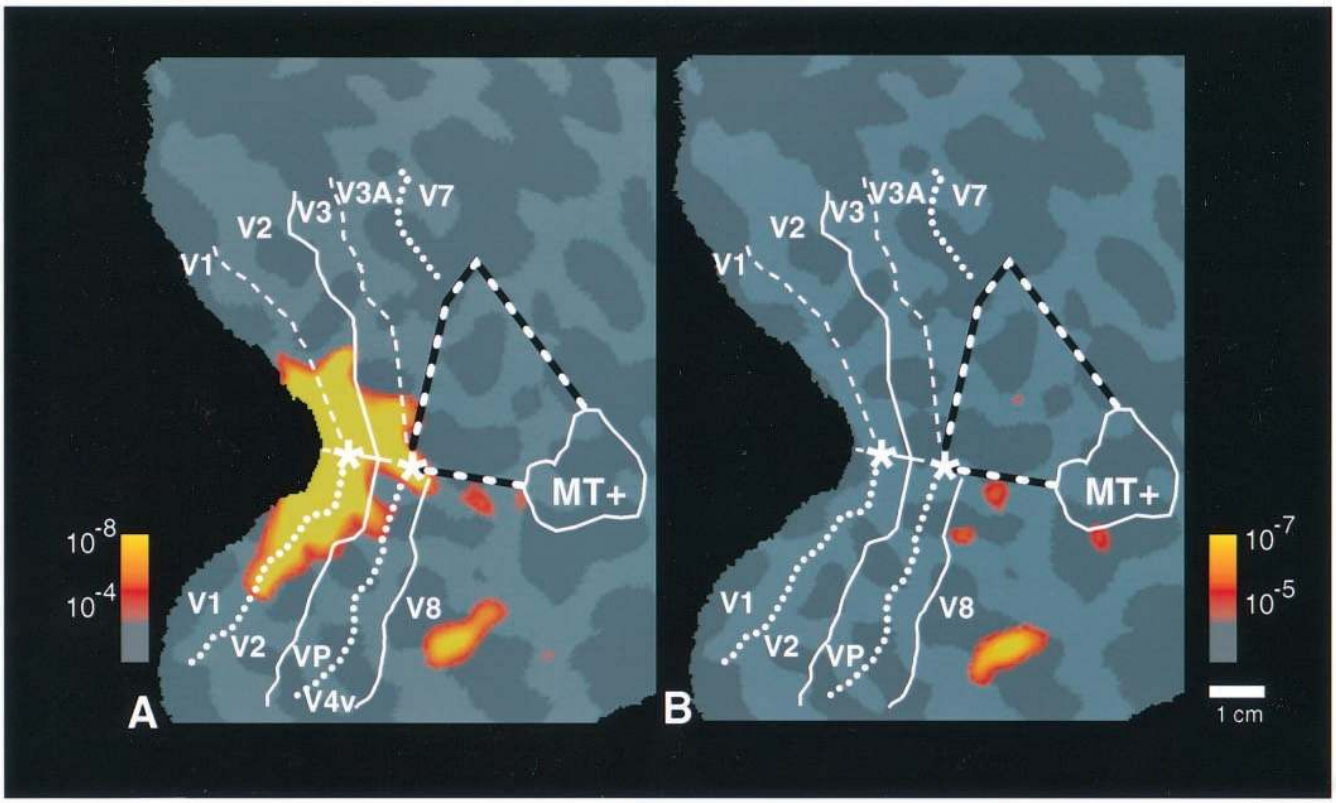

Figure 8

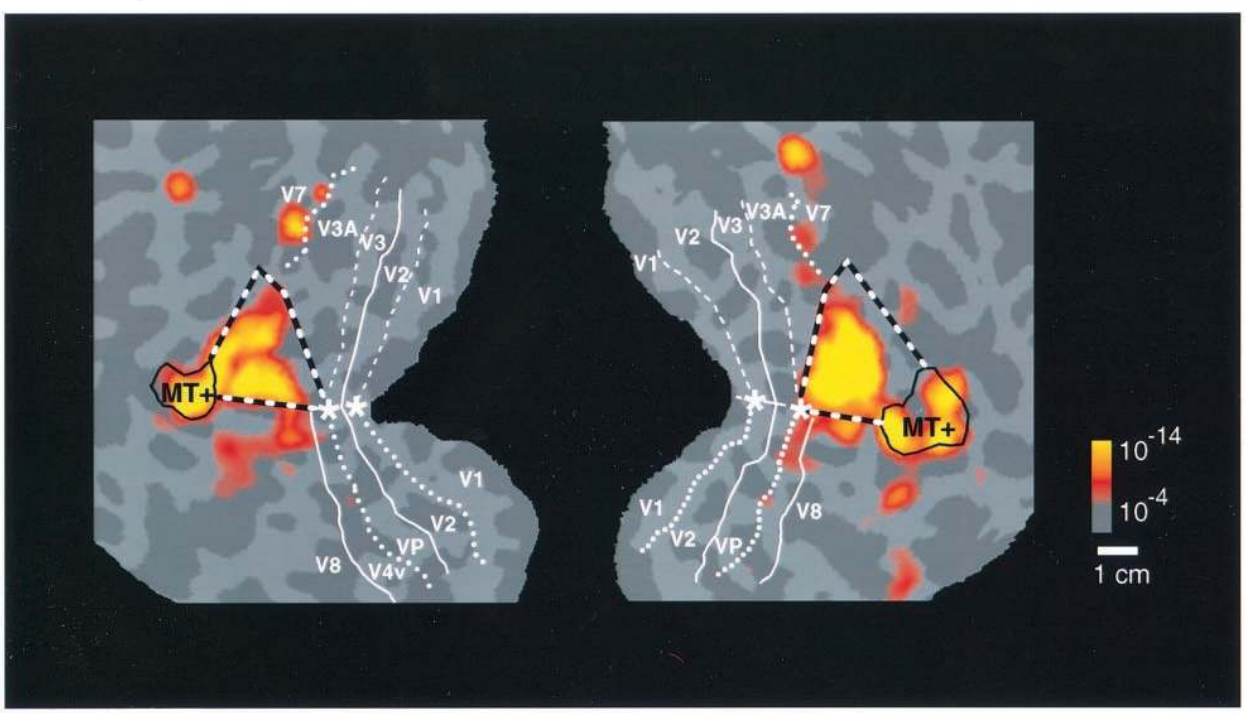

Figure 9

macaque V4d, lie near (but not in) our predicted human V4d topologue? To answer this question, we systematically re-examined the retinotopy of the surrounding cortical areas V3A, V7, V4v and V8. The goal was to consider whether any of those neighboring areas could be the 'missing' V4d homologue, which could have been misinterpreted and/or misnamed previously.

V3A

Here and in previous reports (Tootell *et al*., 1997, 1998; Culham *et al*., 1998; Hasnain *et al*., 1998; Baseler *et al*., 1999; Boynton *et al*., 1999; Mendola *et al*., 1999; Somers *et al*., 1999; Sunaert *et al*., 1999; Wandell, 1999), human V3A encompasses a classical, contiguous representation of the entire contralateral visual field (i.e. 180° of polar angle). The inferior vertical meridian is mapped posteriorly (bordering V3), and the superior vertical meridian is mapped at the anterior border of V3A. The foveal representation is mapped inferiorly, and the periphery is mapped superiorly. These properties of human V3A are generally consistent with those described previously in macaque V3A (see Fig. 1).

Human V3A cannot be a misnamed homologue of V4d, for several reasons. First, V3A includes a contiguous representation of both the upper and lower quadrants of the contralateral visual field (180°), whereas macaque area V4d instead represents just half of that extent (90°). Secondly, macaque V4d is located anterior to V3A. Thus if human V3A was instead the actual homologue of V4d, one would have to somehow explain the absence of human V3A.

V7

Anterior to V3A lies another representation of polar angle that includes (at least) the upper visual field, and is mirror-symmetric to that in anterior V3A. This has been called 'V7' (Tootell *et al*., 1998; Press *et al*., 1999). The representation of eccentricity is not yet clear in V7.

Human 'V7' cannot be a misnamed homologue of macaque V4d because the definitive part of V7 represents the upper visual field, whereas macaque V4d is a representation of the lower visual field. It would only compound the problem of the 'missing V4d' to propose that human V7 (the upper field representation) is the retinotopic counterpart of human V4v (another upper field representation).

Cortical areas can also be distinguished by whether their overall internal retinotopy matches that in the visual field, or whether it is mirror-symmetric to that. This property has been called the field sign, and it is very resistant to evolutionary change (Sereno *et al*., 1994, 1995b). The field sign in V7 is opposite to that found in macaque V4d—so again, V7 cannot be a misnamed V4d.

V4v

The retinotopy and topography of human V4v has been described in several previous reports, with good consensus (Sereno *et al*., 1995a; DeYoe *et al*., 1996; Tootell *et al*., 1997; Van Essen and Drury, 1997; Grill-Spector *et al*., 1998b; Hadjikhani *et al*., 1998; Baseler *et al*., 1999; Wandell, 1999) but see Zeki *et al*. and Bartels and Zeki (Zeki *et al*., 1998; Bartels and Zeki, 2000). In terms of polar angle retinotopy, human V4v is a classical representation of the contralateral upper visual field, with a field sign which is mirror-reversed relative to that in the visual field (i.e. equivalent to that in V2, but opposite to that in V1 and VP) (see Fig. 10). The vertical meridian is represented posteriorly in V4v, along the border with VP. The horizontal meridian forms the anterior boundary of V4v, adjacent to V8. The fovea is represented superiorly in V4v, with increasingly peripheral eccentricities mapped at progressively more inferior locations in cortex. Unlike the anomalous representation of eccentricity in LOC/LOP, the variations in eccentricity representation are quite continuous and orderly in V4v (e.g. Figs 4 and 5).

All these retinotopic features of human V4v are consistent with area V4v as described in macaques (Gattass *et al*., 1988; Van Essen *et al*., 1990; Boussaoud *et al*., 1991; Felleman and Van Essen, 1991a). Thus human 'V4v' cannot be a misnamed 'V4d', for multiple and obvious reasons. For instance, V4v is a representation of the upper visual field, whereas a representation of the lower visual field is required in V4d. Furthermore, if V4v were instead a misnamed 'V4d', then it would be necessary to explain the absence of V4v.

V8

The evidence for an additional retinotopic area which is located immediately anterior to human V4v is described in detail elsewhere (Hadjikhani *et al*., 1998; Wandell, 1999). This area has several names: either 'V8' (Hadjikhani *et al*., 1998); or 'V4' (Lueck *et al*., 1989), or 'VO' (Wandell, 1999). The polar angle retinotopy in V8 is crude (consistent with relatively large receptive fields), but it is consistent across subjects (e.g. Figs 6 and 10).

V8 cannot be an unrecognized or misnamed V4d, for multiple reasons. First, V8 is located ~5.0 cm (center-to-center) from our V4d topologue, based on neighborhood relations in the flattened cortical maps. This is a very long distance across cortex. By comparison, other human retinotopic visual areas (e.g. V2, V3, VP, V4v) are only ~1 cm wide. Thus it could be argued that V8 is separated from our V4d topologue by about four or five 'cortical area equivalents'.

Secondly, V8 includes a coherent representation of both the upper and the lower visual fields, whereas macaque V4d includes a (much larger) representation of the lower visual field.

Figure 8. Neither V4v nor the V4d topologue is significantly color-selective. (*A*) shows the functional activity produced during the comparison of stimuli (radial sine wave gratings), modulated in either luminance or equiluminant color. The orange–red regions were preferentially activated by the color-varying stimuli. This activated region includes mostly the foveal representation of the classically retinotopic areas (e.g. V1, V2, V3/VP, etc.). However, an additional small area was also activated in ventral cortex, in the depth of the collateral sulcus, anterior to retinotopically defined V4v. We call this ventral color-selective area 'V8' (Hadjikhani *et al*., 1998), but the apparently identical area was previously called 'V4'. It corresponds to the cortical region indicated by the pinwheel color logo in Figures 2 and 3. (*B*) shows activation in V8 of the same subject, produced by the percept of a color afterimage on a uniform gray stimulus. In this stimulus comparison, the pattern of activation is much more selective for V8. Area V8 is a long distance (~5cm, center-to-center) across the cortical surface from the V4d topologue.

Figure 9. Functional selectivity in the V4d topologue differs from that in V4v. This figure shows the activity produced by viewing of kinetic motion boundaries embedded in random dot stimuli, compared with viewing otherwise identical, transparently moving random dot stimuli lacking motion boundaries. For ease of comparison, it is shown from the same subject illustrated in Figure 8, but here the patterns are shown in both left and right hemispheres, on the left and right of the figure, respectively. Consistent with earlier reports, the kinetic motion boundaries produced high relative activity in a region located between V3A, V4v and MT+—exactly where the V4d topologue is located. This functionally defined area has been called 'KO' (Orban *et al*., 1995; Dupont *et al*., 1997; Van Oostende *et al*., 1997). Here, increased activity produced by kinetic boundaries was also higher in MT+.

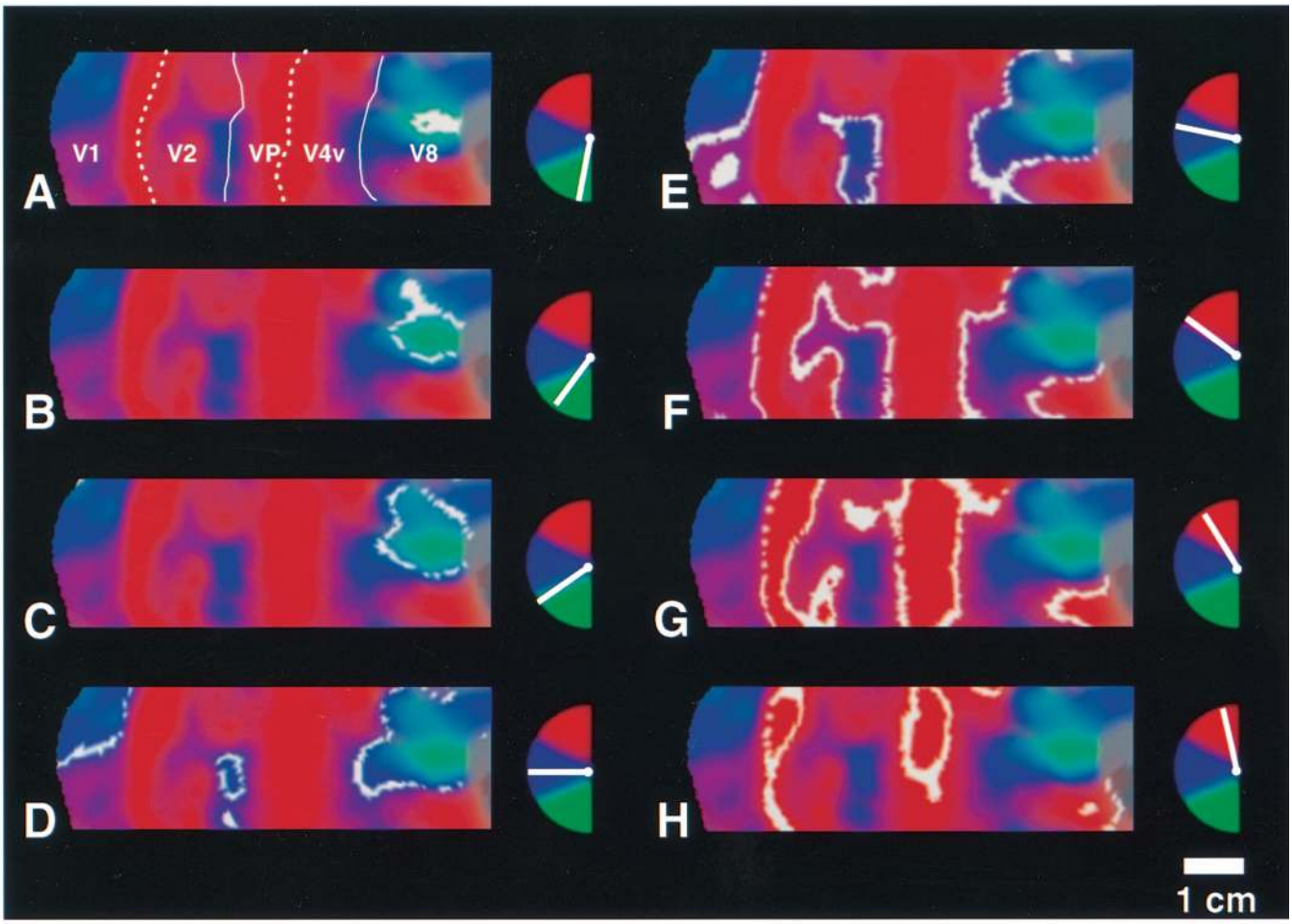

Figure 10. Detailed polar angle retinotopy of V4v, V8 and neighboring areas. This figure shows the peak fMRI response (noisy white lines) corresponding to retinotopic polar angle differences of ~20°, superimposed on the standard pseudocolor rendering of areas V1, V2, VP and V4v, indicated in (*A*). To the right of each panel is a logo indicating the stimulus polar angle (white line). The complete contralateral visual field is represented in V8, from the lower visual field (*A*,*B*), across the horizontal meridian (*C*–*E*), to the upper visual field (*F*–*H*). In contrast, V4v includes only a representation of the upper visual field (*E*–*H*). The upper visual field representations in V4v and V8 are of opposing field sign and can be clearly distinguished in this high-resolution data (*E*–*H*).

Thirdly, the foveal representation of V8 lies at its anterior edge, several centimeters from the foveal representation in V4v. Fourth, the field sign in V8 is opposite to that in V4v, so logically V4v and V8 cannot be parts of the same visual area (see Fig. 9).

The original rationale for referring to this small human area (V8) as 'V4' is that this area shows some color selectivity (e.g. Fig. 8). However, since the original claims of color selectivity in macaque V4d have not been confirmed, this original rationale is moot.

The border between 'V8' and 'V4v' is somewhat unusual, since it is not a simple mirror-reversal of polar angle. In data with adequate signal-to-noise, this representation of the (horizontal) meridian is perfectly straightforward (e.g. Fig. 10). However with less robust data, and/or lower polar angle resolution (e.g. pseudocolor only), the horizontal meridian at the anterior border of V4v can be somewhat subtle.

Talairach Coordinates

The Talairach coordinates of the original ventral color-selective region ('V8' or 'V4' or 'VO') were never in dispute, although this has been a matter of apparent confusion (Zeki *et al.*, 1998; Bartels and Zeki, 2000). In fact, there has been fairly good agreement in these coordinates across different studies, with average coordinates near +/–26, –67, –9. However, the averaged coordinates of our V4d topologue were quite different (+/–41.25; –81; 8). This supports all the other evidence that the ventral color-selective area is not the human homologue of area V4(d).

Functional Tests in V4d

In prior fMRI studies, the V4d topologue was not explicitly defined as we have done here. Nevertheless, the approximate location of the V4d topologue can be estimated *post hoc* in those studies that illustrated the boundaries of V3A, V4v and MT+. Such retrospective analysis reveals that the V4d topologue responds well in a wide range of stimulus comparisons that require information processing across relatively large regions of the visual field. Such examples include tests of illusory contours (Mendola *et al.*, 1999), object recognition (Grill-Spector *et al.*, 1998a,b), and visual symmetry (Tyler and Baseler, 1997). A specialization for kinetic motion processing (e.g. Fig. 9) may also require processing across a relatively large region of the visual field. Such a conclusion is consistent with other evidence that the receptive fields in the V4d topologue (i.e. LOC and LOP) are relatively large and non-retinotopic (Tootell *et al.*, 1997).

Neither of the human 'V4' subdivisions had unusually high

color sensitivity, in the tests we performed so far (e.g. Fig. 8). In that sense, the functional activity in human 'V4' was unlike that described in early reports from macaque V4 (Zeki, 1973, 1977, 1983).

Implications for Macaque V4

The present fMRI data brings up another possibility: perhaps macaque V4d is actually more like its human counterpart than previously recognized. This would be easy to rationalize *post hoc*. The receptive fields in macaque V4d tend to be large and sometimes poorly defined, and electrophysiological retinotopic maps are (by necessity) highly under-sampled. Similarly, retinotopic maps based on neural tracers are usually extrapolations based on one or just a few injections, often across animals. If one is trying to extrapolate maps of an expected continuous, and classical retinotopic map from such data, one could easily miss the unusual retinotopic features revealed by the fMRI in LOC/LOP.

In fact, there is some support for this idea. Even the early studies of Zeki (Zeki, 1977) concluded that 'this [V4d] is not a homogeneous region but [sic] can be subdivided into separate anatomical and functional domains', and described it as a 'complex' of different sub-regions such as the transiently proposed 'V4A' (Zeki, 1977). The early retinotopic mapping studies of Maguire and Bazier (Baizer and Maguire, 1983; Maguire and Baizer 1984) also concluded that multiple retinotopic areas could be distinguished, along a border which lay approximately where the LOC/LOP border would lie in macaque. Even the most well-documented electrophysiological mapping study of V4d (Gattass *et al*., 1988) shows clear receptive field discontinuities, also near where the LOC/LOP border should be located in macaque.

Subsequent tracer studies by Kaas and co-workers strongly suggest that area DL [which was originally considered homologous to V4d (Baker *et al*., 1981)], is in fact subdivided into two adjacent areas, based partly on retinotopic eccentricity (DL rostral and DL caudal) along a border similar to that separating human LOC from LOP (Cusick and Kaas, 1988; Steele *et al*., 1991; Weller *et al*., 1991; Stepniewska and Kaas, 1996). Cumulatively, all this data suggests that subdivisions similar to LOC/LOP may exist in some species of non-human primates, as well as in humans.

With hindsight, it can even be argued that 'V4v' should *never* have been considered a match to 'V4d', even in the macaque. To begin with, the shape and size of the two subdivisions are quite different: 'V4d' is large and irregularly circular in shape, whereas 'V4v' is topographically long and thin. Thus these two 'V4' subdivisions are not mirror-symmetrical, in the way that the more classic quarter-field representations are laid out in V2d/V2v, and in adjacent area(s) V3d/V3v (also known as V3/VP) (see Fig. 1). Since the topographical shape of an area directly reflects its internal retinotopy, this difference in the shape and size of V4d and V4v should have prompted reconsideration of the V4d/V4v 'marriage' long ago.

It may also be noteworthy that there were so many discrepancies in the electrophysiological descriptions of the polar angle retinotopy in macaque V4d: each report differed significantly from the others (Maguire and Baizer, 1984; Gattass *et al*., 1988; Boussaoud *et al*., 1991). One simple interpretation is that the polar angle retinotopy in V4d is not well organized, or it may be variable between individuals—as we found in our human studies (e.g. Figs 6 and 7). If this were true in macaque V4d, then obviously different investigators, working on different monkeys, would find and report correspondingly different retinotopy in this region.

Of course, it could be argued that the discrepancies between the earlier data and the present data arise not from species differences, but from differences in the techniques used to map the retinotopy. Macaque V4 was mapped using single unit electrophysiology, a relatively direct measure of neural activity. On the other hand, the human retinotopy has been mapped using fMRI—a technique with complementary advantages and disadvantages (more complete coverage of visual cortex, based on hemodynamic reflections of neural activity). In other retinotopic areas (e.g. V1, V2, V3, VP, V3A, V4v), similar comparisons between macaques and human retinotopy using these same techniques have matched very well. Therefore, the present differences are not likely due to trivial technical differences. Retinotopic mapping experiments using fMRI in awake behaving macaques (now underway) will presumably resolve this issue.

Although we have tried hard to interpret the mapping data correctly, the present conclusions leave us with one major unresolved question: where is the lower-field representation that can serve as a retinotopic and functional counterpart to area 'V4v'? Unfortunately we do not yet know the answer. Although such 'separated' quarter-field representations are conceptually unsatisfying, they are not unprecedented: the quarter-field representations in macaque 'V3' and 'VP' have long been considered separate areas by some investigators, based on empirical differences between V3 and VP (Burkhalter *et al*., 1986; Van Essen *et al*., 1986; Felleman and Van Essen, 1991b; Felleman *et al*., 1997). We hope that this apparent asymmetry will be clarified with the passage of time, improvements in cortical mapping technology, and better understanding of the principles underlying cortical mapping.

Notes

These experiments were supported by grant no. EY07980 to R.B.H.T. We thank Dr Guy Orban for generously furnishing copies of the kinetic boundary stimuli, and Anders Dale, Bruce Fischl and Arthur Liu for use of the cortical flattening code.

Address correspondence to Roger B.H. Tootell, Nuclear Magnetic Resonance Center, Department of Radiology, Massachusetts General Hospital, Charlestown, MA 02129, USA. Email: tootell@nmr.mgh.harvard.edu.

References

Allman JM, Kaas JH (1976) Representation of the visual field on the medical wall of occipital–parietal cortex in the owl monkey. Science 191:572–575.

Andersen RA, Asanuma C, Cowan WM (1985) Callosal and prefrontal associational projecting cell populations in area 7A of the macaque monkey: a study using retrogradely transported fluorescent dyes. J Comp Neurol 232:443–455.

Baizer JS, Maguire WM (1983) Double representation of lower visual quadrant in prelunate gyrus of rhesus monkey. Invest Ophthalmol Vis Sci 24:1436–1439.

Baker JF, Petersen SE, Newsome WT, Allman JM (1981) Visual response properties of neurons in four extrastriate visual areas of the owl monkey (*Aotus trivirgatus*): a quantitative comparison of medial, dorsomedial, dorsolateral, and middle temporal areas. J Neurophysiol 45:397–416.

Bar M, Biederman I (1999) Localizing the cortical region mediating visual awareness of object identity. Proc Natl Acad Sci USA 96:1790–1793.

Bartels A, Zeki S (2000) The architecture of the colour centre in the human visual brain: new results and a review. Eur J Neurosci 12: 172–193.

Baseler HA, Morland AB, Wandell BA (1999) Topographic organization of

human visual areas in the absence of input from primary cortex. J Neurosci 19:2619–2627.
Beauchamp MS, Haxby JV, Jennings JE, DeYoe EA (1999) An fMRI version of the Farnsworth–Munsell 100–Hue test reveals multiple color-selective areas in human ventral occipitotemporal cortex. Cereb Cortex 9:257–263.
Boussaoud D, Desimone R, Ungerleider LG (1991) Visual topography of area TEO in the macaque. J Comp Neurol 306:554–575.
Boynton GM, Demb JB, Glover GH, Heeger DJ (1999) Neuronal basis of contrast discrimination. Vision Res 39:257–269.
Burkhalter A, Felleman DJ, Newsome WT, Van Essen DC (1986) Anatomical and physiological asymmetries related to visual areas V3 and VP in macaque extrastriate cortex. Vision Res 26:63–80.
Cheng K, Hasegawa T, Saleem KS, Tanaka K (1994) Comparison of neuronal selectivity for stimulus speed, length, and contrast in the prestriate visual cortical areas V4 and MT of the macaque monkey. J Neurophysiol 71:2269–2280.
Colby CL, Duhamel JR (1991) Heterogeneity of extrastriate visual areas and multiple parietal areas in the macaque monkey. Neuropsychologia 29:517–537.
Connor CE, Gallant JL, Preddie DC, Van Essen DC (1996) Responses in area V4 depend on the spatial relationship between stimulus and attention. J Neurophysiol 75:1306–1308.
Connor CE, Preddie DC, Gallant JL, Van Essen DC (1997) Spatial attention effects in macaque area V4. J Neurosci 17:3201–3214.
Courtney SM, Finkel LH, Buchsbaum G (1995) Network simulations of retinal and cortical contributions to color constancy. Vision Res 35:413–434.
Culham JC, Brandt SA, Cavanagh P, Kanwisher NG, Dale AM, Tootell RB (1998) Cortical fMRI activation produced by attentive tracking of moving targets. J Neurophysiol 80:2657–2670.
Cusick CG, Kaas JH (1988) Cortical connections of area 18 and dorsolateral visual cortex in squirrel monkeys. Vis Neurosci 1: 211–237.
Dale AM, Fischl B, Sereno MI (1999) Cortical surface-based analysis I: Segmentation and surface reconstruction. NeuroImage 9:179–194.
Daniel PM, Whitteridge D (1961) The representation of the visual field on the cerebral cortex of monkeys. J Physiol 159:203–221.
Desimone R, Schein SJ (1987) Visual properties of neurons in area V4 of the macaque: sensitivity to stimulus form. J Neurophysiol 57:835–868.
DeYoe EA, Carman GJ, Bandettini P, Glickman S, Wieser J, Cox R, Miller D, Neitz J (1996) Mapping striate and extrastriate visual areas in human cerebral cortex. Proc Natl Acad Sci USA 93:2382–2386.
Dupont P, De Bruyn B, Vandenberghe R, Rosier AM, Michiels J, Marchal G, Mortelmans L, Orban GA (1997) The kinetic occipital region in human visual cortex. Cereb Cortex 7:283–292.
Engel SA, Rumelhart DE, Wandell BA, Lee AT, Glover GH, Chichilnisky EJ, Shadlen MN (1994) fMRI of human visual cortex. Nature 369:525.
Engel SA, Glover GH, Wandell BA (1997) Retinotopic organization in human visual cortex and the spatial precision of functional MRI. Cereb Cortex 7:181–192.
Felleman DJ, Van Essen DC (1991a) Distributed hierarchical processing in primate cerebral cortex. Cerebral Cortex 1:1–47.
Felleman DJ, Van Essen DC (1991b) Distributed hierarchical processing in the primate cerebral cortex. Cereb Cortex 1:1–47.
Felleman DJ, Burkhalter A, Van Essen DC (1997) Cortical connections of areas V3 and VP of macaque monkey extrastriate visual cortex. J Comp Neurol 379:21–47.
Ferrera VP, Nealey TA, Maunsell JH (1992) Mixed parvocellular and magnocellular geniculate signals in visual area V4. Nature 358: 756–761.
Ferrera VP, Nealey TA, Maunsell JH (1994) Responses in macaque visual area V4 following inactivation of the parvocellular and magnocellular LGN pathways. J Neurosci 14:2080–2088.
Fischer B, Boch R, Bach M (1981) Stimulus versus eye movements: comparison of neural activity in the striate and prelunate visual cortex (A17 and A19) of trained rhesus monkey. Exp Brain Res 43:69–77.
Fischl B, Sereno MI, Dale AM (1999) Cortical surface-based analysis II: Inflation, flattening, and a surface-based coordinate system. NeuroImage 9:195–207.
Gallant JL, Braun J, Van Essen DC (1993) Selectivity for polar, hyperbolic, and Cartesian gratings in macaque visual cortex. Science 259: 100–103.
Gattass R, Sousa AP, Gross CG (1988) Visuotopic organization and extent of V3 and V4 of the macaque. J Neurosci 8:1831–1845.
Gochin PM (1994) Properties of simulated neurons from a model of primate inferior temporal cortex. Cereb Cortex 4:532–543.
Grill-Spector K, Kushnir T, Edelman S, Itzchak Y, Malach R (1998a) Cue-invariant activation in object-related areas of the human occipital lobe. Neuron 21:191–202.
Grill-Spector K, Kushnir T, Hendler T, Edelman S, Itzchak Y, Malach R (1998b) A sequence of object-processing stages revealed by fMRI in the human occipital lobe. Hum Brain Mapp 6:316–328.
Hadjikhani N, Liu AK, Dale AM, Cavanagh P, Tootell RBH (1998) Retinotopy and color selectivity in human visual cortical area V8. Nat Neurosci 1:235–241.
Haenny PE, Maunsell JH, Schiller PH (1988) State dependent activity in monkey visual cortex. II. Retinal and extraretinal factors in V4. Exp Brain Res 69:245–259.
Hasnain MK, Fox PT, Woldorff MG (1998) Intersubject variability of functional areas in the human visual cortex. Hum Brain Mapp 6:301–315.
Heywood CA, Gadotti A, Cowey A (1992) Cortical area V4 and its role in the perception of color. J Neurosci 12:4056–4065.
Heywood CA, Gaffan D, Cowey A (1995) Cerebral achromatopsia in monkeys. Eur J Neurosci 7:1064–1073.
Hubel DH, Wiesel TN (1974) Uniformity of monkey striate cortex: a parallel relationship between field size, scatter, and magnification factor. J Comp Neurol 158:295–305.
Kaas JH (1995) Human visual cortex. Progress and puzzles. Curr Biol 5:1126–1128.
Kaas JH, Krubitzer LA (1991) In: Neuroanatomy of visual pathways and their retinotopic organization (Dreher B, Robinson SR, eds), pp. 302–359. London: Macmillan.
Kaas JH, Morel A (1993) Connections of visual areas of the upper temporal lobe of owl monkeys: the MT crescent and dorsal and ventral subdivisions of FST. J Neurosci 13:534–546.
Lueck CJ, Zeki S, Friston KJ, Deiber MP, Cope P, Cunningham VJ, Lammertsma AA, Kennard C, Frackowiak RS (1989) The colour centre in the cerebral cortex of man. Nature 340:386–389.
Maguire WM, Baizer JS (1984) Visuotopic organization of the prelunate gyrus in rhesus monkey. J Neurosci 4:1690–1704.
Maunsell JH, Newsome WT (1987) Visual processing in monkey extrastriate cortex. Annu Rev Neurosci 10:363–401.
May JG, Andersen RA (1986) Different patterns of corticopontine projections from separate cortical fields within the inferior parietal lobule and dorsal prelunate gyrus of the macaque. Exp Brain Res 63:265–278.
McAdams CJ, Maunsell JH (2000) Attention to both space and feature modulates neuronal responses in macaque area V4. J Neurophysiol 83:1751–1755.
Mendola J, Dale AM, Fischl B, Liu AK, Tootell RBH (1999) The representation of illusory and real contours in human cortical visual areas revealed byfunctional magnetic resonance imaging. J. Neurosci 19:8560–8572.
Moran J, Desimone R (1985) Selective attention gates visual processing in the extrastriate cortex. Science 229:782–784.
Motter BC (1993) Focal attention produces spatially selective processing in visual cortical areas V1, V2, and V4 in the presence of competing stimuli. J Neurophysiol 70:909–919.
Niebur E, Koch C (1994) A model for the neuronal implementation of selective visual attention based on temporal correlation among neurons. J Comput Neurosci 1:141–158.
Orban GA, Dupont P, De Bruyn B, Vogels R, Vandenberghe R, Mortelmans L (1995) A motion area in human visual cortex. Proc Natl Acad Sci USA 92:993–997.
Press W, Dougherty R, Wandell B (1999) Contour integration in human retinotopic visual areas. Soc Neurosci Abstr 25:1163.
Rosa MG, Krubitzer LA (1999) The evolution of visual cortex: where is V2? Trends Neurosci 22:242–248.
Rosa MG, Soares JG, Fiorani M Jr, Gattass R (1993) Cortical afferents of visual area MT in the Cebus monkey: possible homologies between New and Old World monkeys. Vis Neurosci 10:827–855.
Salinas E, Abbott LF (1997) Invariant visual responses from attentional gain fields. J Neurophysiol 77:3267–3272.
Schein SJ, Desimone R (1990) Spectral properties of V4 neurons in the macaque. J Neurosci 10:3369–3389.
Schein SJ, Marrocco RT, de Monasterio FM (1982) Is there a high concentration of color-selective cells in area V4 of monkey visual cortex? J Neurophysiol 47:193–213.

Schiller PH (1993) The effects of V4 and middle temporal (MT) area lesions on visual performance in the rhesus monkey. Vis Neurosci 10:717–746.
Sereno MI, Allman JM (1991) In: The neural basis of visual function (Leventhal AG, ed.), pp. 160–172. London: Macmillan.
Sereno MI, McDonald CT, Allman JM (1994) Analysis of retinotopic maps in extrastriate cortex. Cereb Cortex 4:601–620.
Sereno MI, Dale AM, Reppas JB, Kwong KK, Belliveau JW, Brady TJ, Rosen BR, Tootell RB (1995a) Borders of multiple visual areas in humans revealed by functional magnetic resonance imaging [see comments]. Science 268:889–893.
Sereno MI, Dale AM, Reppas JB, Kwong KK, Belliveau JW, Brady TJ, Rosen BR, Tootell RBH (1995b) Borders of multiple visual areas in humans revealed by functional magnetic resonance imaging. Science 268:889–893.
Somers DC, Dale AM, Seiffert AE, Tootell RB (1999) Functional MRI reveals spatially specific attentional modulation in human primary visual cortex. Proc Natl Acad Sci USA 96:1663–1668.
Steele GE, Weller RE, Cusick CG (1991) Cortical connections of the caudal subdivision of the dorsolateral area (V4) in monkeys. J Comp Neurol 306:495–520.
Stepniewska I, Kaas JH (1996) Topographic patterns of V2 cortical connections in macaque monkeys. J Comp Neurol 371:129–152.
Sunaert S, Van Hecke P, Marchal G, Orban GA (1999) Motion-responsive regions of the human brain. Exp Brain Res 127:355–370.
Takechi H, Onoe H, Shizuno H, Yoshikawa E, Sadato N, Tsukada H, Watanabe Y (1997) Mapping of cortical areas involved in color vision in non-human primates. Neurosci Lett 230:17–20.
Talairach J, Tournoux P (1988) Co-planar stereotaxic atlas of the human brain. New York: Thieme Medical Publishers.
Tootell RBH, Hadjikhani N (1998) Has a new color area been discovered? (reply). Nat Neurosci 1:335–336.
Tootell RB, Taylor JB (1995) Anatomical evidence for MT and additional cortical visual areas in humans. Cereb Cortex 5:39–55.
Tootell RB, Hamilton SL, Silverman MS (1985) Topography of cytochrome oxidase activity in owl monkey cortex. J Neurosci 5:2786–2800.
Tootell RB, Switkes E, Silverman MS, Hamilton SL (1988) Functional anatomy of macaque striate cortex. II. Retinotopic organization. J Neurosci 8:1531–1568.
Tootell RBH, Reppas JB, Kwong KK, Malach R, Born RT, Brady TJ, Rosen BR, Belliveau JW (1995) Functional analysis of human MT and related visual cortical areas using magnetic resonance imaging. J Neurosci 15:3215–3230.
Tootell RB, Mendola JD, Hadjikhani NK, Ledden PJ, Liu AK, Reppas JB, Sereno MI, Dale AM (1997) Functional analysis of V3A and related areas in human visual cortex. J Neurosci 17:7060–7078.
Tootell RBH, Hadjikhani N, Hall EK, Marrett S, Vanduffel W, Vaughan JT, Dale AM (1998) The retinotopy of visual spatial attention. Neuron 21: 1409–1422.
Tyler C, Baseler H (1997) FMRI signals from a cortical region specific for multiple pattern symmetries (abstract). IOVS 39:s169.
Van Essen DC (1997) A tension-based theory of morphogenesis and compact wiring in the central nervous system. Nature 385:313–318.
Van Essen DC, Drury HA (1997) Structural and functional analyses of human cerebral cortex using a surface-based atlas. J Neurosci 17:7079–7102.
Van Essen DC, Gallant JL (1994) Neural mechanisms of form and motion processing in the primate visual system. Neuron 13:1–10.
Van Essen DC, Zeki SM (1978) The topographic organization of rhesus monkey prestriate cortex. J Physiol (Lond) 277:193–226.
Van Essen DC, Newsome WT, Maunsell JH (1984) The visual field representation in striate cortex of the macaque monkey: asymmetries, anisotropies, and individual variability. Vision Res 24:429–448.
Van Essen DC, Newsome WT, Maunsell JH, Bixby JL (1986) The projections from striate cortex (V1) to areas V2 and V3 in the macaque monkey: asymmetries, areal boundaries, and patchy connections. J Comp Neurol 244:451–480.
Van Essen DC, Felleman DJ, DeYoe EA, Olavarria J, Knierim J (1990) Modular and hierarchical organization of extrastriate visual cortex in the macaque monkey. Cold Spring Harb Symp Quant Biol 55:679–696.
Van Essen D, Anderson C, Felleman D (1992) Information processing in the primate visual system: an integrated systems perspective. Science 255:419–423.
Van Essen DC, Lewis JW, Drury HA, Hadjikhani N, Tootell RBH, Bakircioglu M, Miller MI (2000) Mapping visual cortex in monkeys and humans using surface-based atlases. Vision Research, submitted.
Van Oostende S, Sunaert S, Van Hecke P, Marchal G, Orban GA (1997) The kinetic occipital (KO) region in man: an fMRI study. Cereb Cortex 7:690–701.
Wachtler T, Albright TD, Sejnowski TJ (1997) Spatial interactions in color perception. Invest Ophthalmol Vis Sci 38:898.
Wachtler T, Albright TD, Sejnowski TJ (1998) Non-local color induction under changing adaptation depends on chromatic contrast. Soc Nerosci Abstr 24:1398.
Wachtler T, Sejnowski TJ, Albright TD (1999a) Interactions between stimulus and background chromaticities in macaque primary visual cortex. Invest Ophthalmol Vis Sci 40:641.
Wachtler T, Sejnowski TJ, Albright TD (1999b) Responses of cells in macaque V1 to chromatic stimuli are compatible with human color constancy. Soc Neurosci Abstr 25:4.
Walsh V, Carden D, Butler SR, Kulikowski JJ (1993) The effects of V4 lesions on the visual abilities of macaques: hue discrimination and colour constancy. Behav Brain Res 53:51–62.
Wandell BA (1999) Computational neuroimaging of human visual cortex. Annu Rev Neurosci 22:145–173.
Watson JD, Myers R, Frackowiak RS, Hajnal JV, Woods RP, Mazziotta JC, Shipp S, Zeki S (1993) Area V5 of the human brain: evidence from a combined study using positron emission tomography and magnetic resonance imaging. Cereb Cortex 3:79–94.
Weller RE, Steele GE, Cusick CG (1991) Cortical connections of dorsal cortex rostral to V II in squirrel monkeys. J Comp Neurol 306: 521–537.
Wilson HR, Krupa B, Wilkinson F (2000) Dynamics of perceptual oscillations in form vision. Nat Neurosci 3:170–176.
Zeki S (1983) The distribution of wavelength and orientation selective cells in different areas of monkey visual cortex. Proc R Soc Lond B Biol Sci 217:449–470.
Zeki S, McKeefry DJ, Bartels A, Frackowiak RS (1998) Has a new color area been discovered? Nat Neurosci 1:335–336.
Zeki S, Watson JDG, Lueck CJ, Friston KJ, Kennard C, Frackowiak RSJ (1991) A direct demonstration of functional specialization in human visual cortex. J Neurosci 11:641–649.
Zeki SM (1973) Colour coding in rhesus monkey prestriate cortex. Brain Res 53:422–427.
Zeki SM (1977) Colour coding in the superior temporal sulcus of rhesus monkey visual cortex. Proc R Soc Lond B Biol Sci 197:195–223.
Zeki SM (1978) Uniformity and diversity of structure and function in rhesus monkey prestriate visual cortex. J Physiol (Lond) 277:273–290.